Reduction of the Position Bias via Multi-Level Learning for Activity Recognition

#417

Aomar Osmani **Massinissa Hamidi**
LIPN-UMR CNRS 7030, Univ. Sorbonne Paris Nord

PAKDD 2022
THE 26TH PACIFIC-ASIA CONFERENCE ON KNOWLEDGE DISCOVERY AND DATA MINING
MAY, 16-19 CHENGDU, CHINA

Université Sorbonne Paris Nord

Activity Recognition from Sensor Deployments

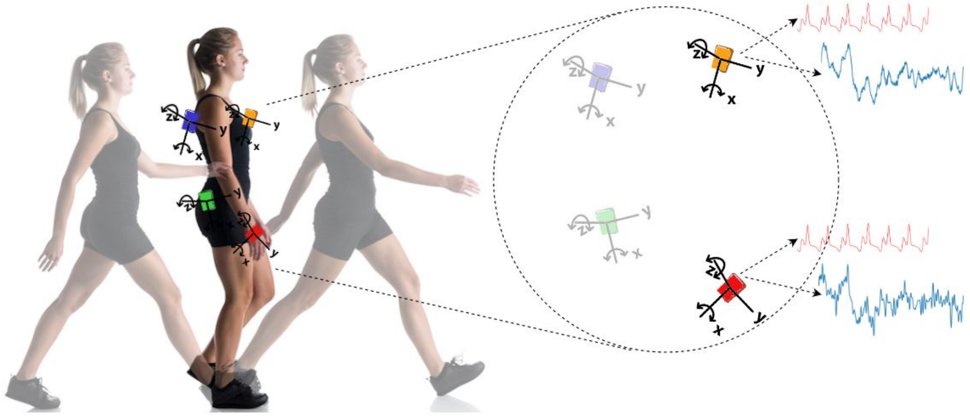

Activity Recognition from Sensor Deployments

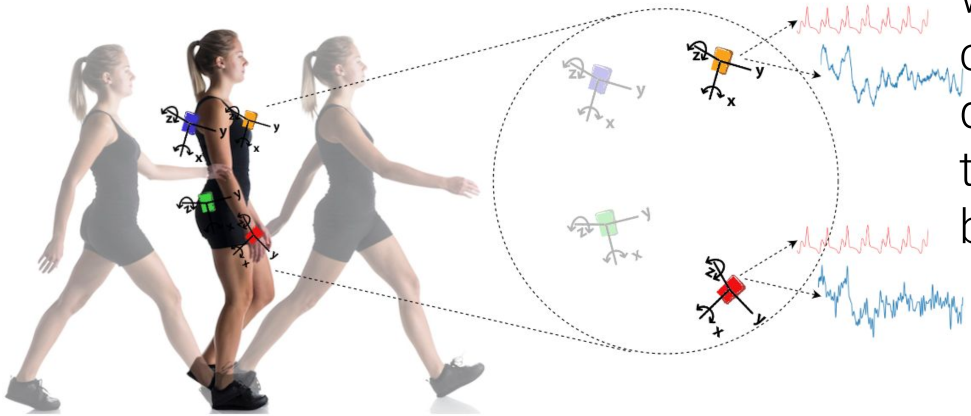

we consider configurations where a collection $\mathcal{S}$ of M sensors, denoted $\{s_1, \ldots, s_M\}$, is deployed on the object of interest (e.g., human body) at the positions $\{p_1, \ldots, p_M\}$.

Activity Recognition from Sensor Deployments

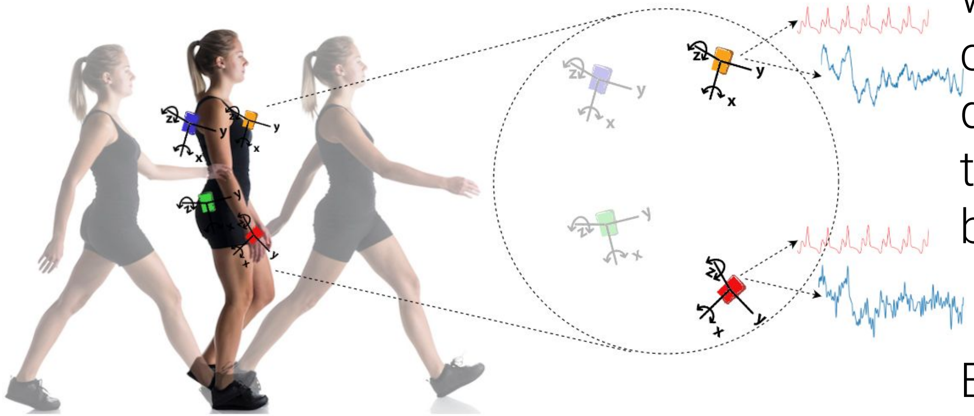

we consider configurations where a collection $\mathcal{S}$ of M sensors, denoted $\{s_1, \ldots, s_M\}$, is deployed on the object of interest (e.g., human body) at the positions $\{p_1, \ldots, p_M\}$.

Each sensor s_i generates a stream $\mathbf{x}^i = (x_1^i, x_2^i, \ldots)$ of observations of a certain modality such as acceleration or gravity.

Activity Recognition from Sensor Deployments

- Acc, Gyr, Mag, etc.;
- Time-series;

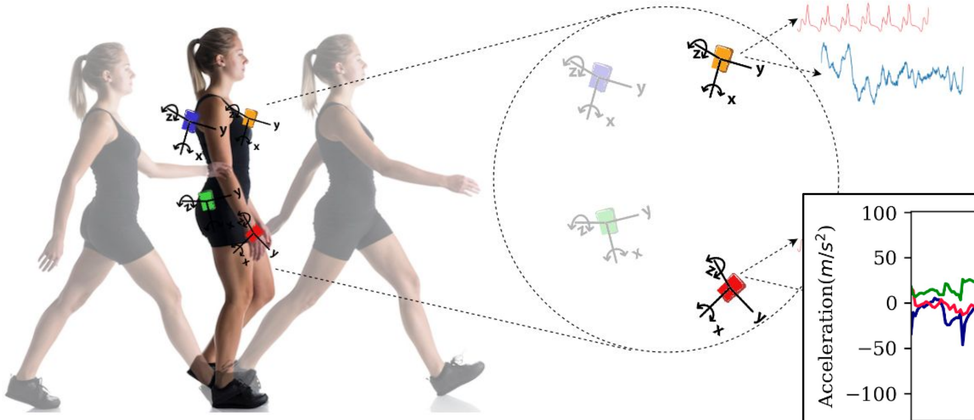

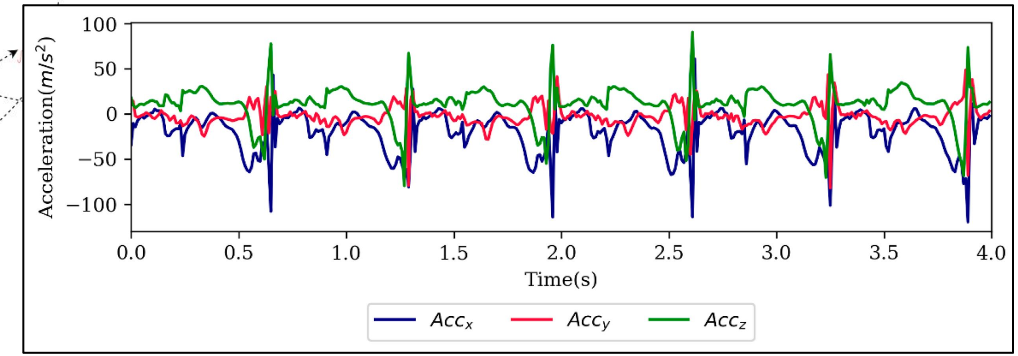

Activity Recognition from Sensor Deployments

- Acc, Gyr, Mag, etc.;
- Time-series;
- Segmentation (segment size, overlapping coefficient, etc.);

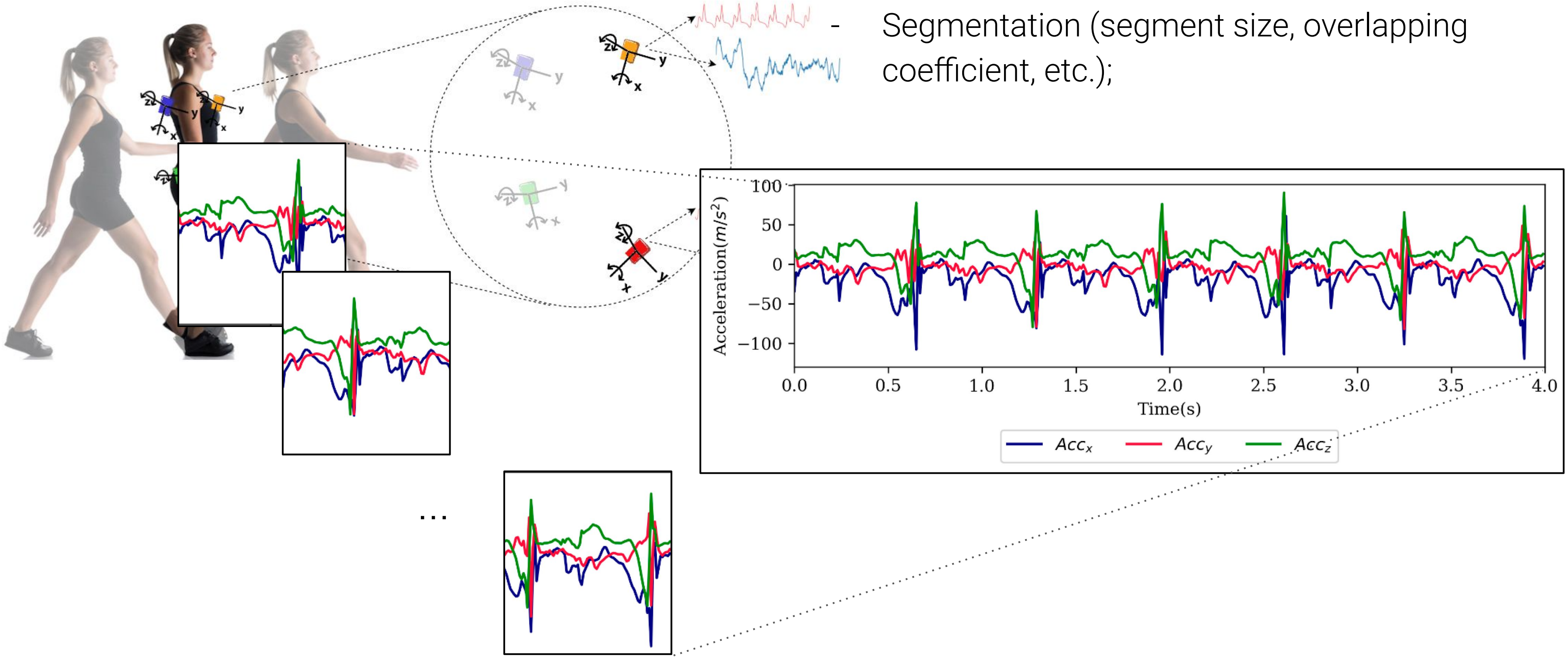

Activity Recognition from Sensor Deployments

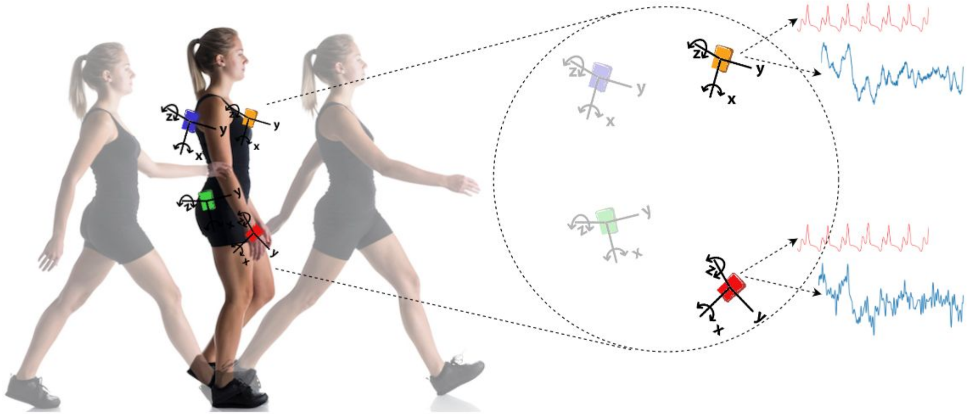

- Acc, Gyr, Mag, etc.;
- Time-series;

Segmentation (segment size, overlapping coefficient, etc.);

Generally, we cast this problem as a sequence classification task (using, e.g., neural networks, responsible for extracting relevant characteristics from the signal, etc.;

LSTMs are used to model the temporal dependencies of the signal;

Activity Recognition from Sensor Deployments

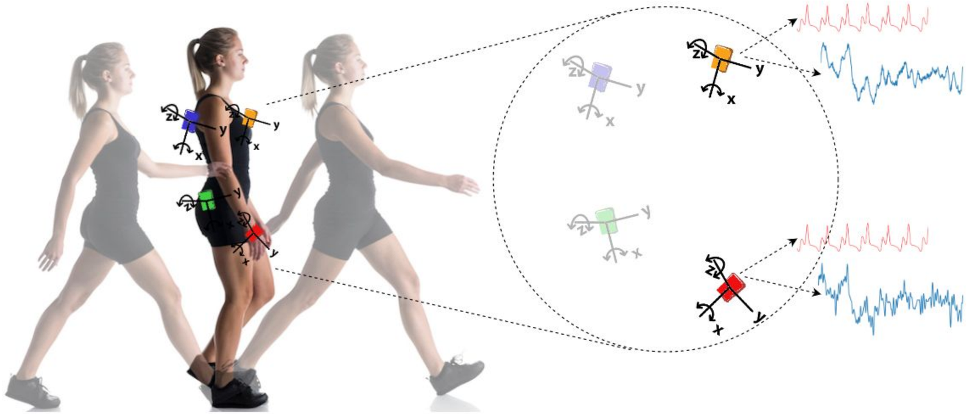

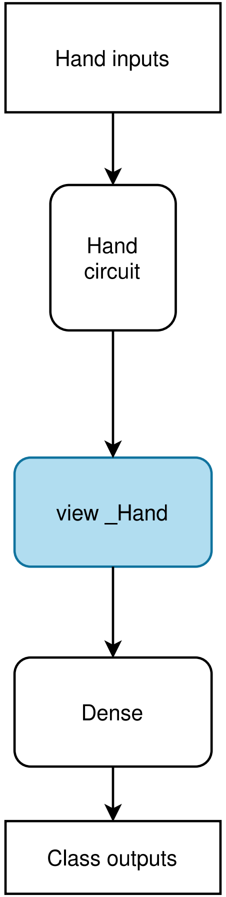

Bias Induced by the Sensor's Position

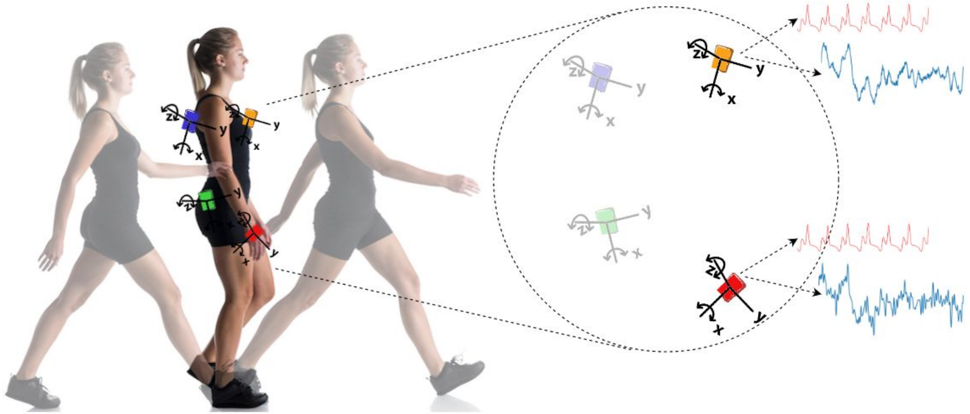

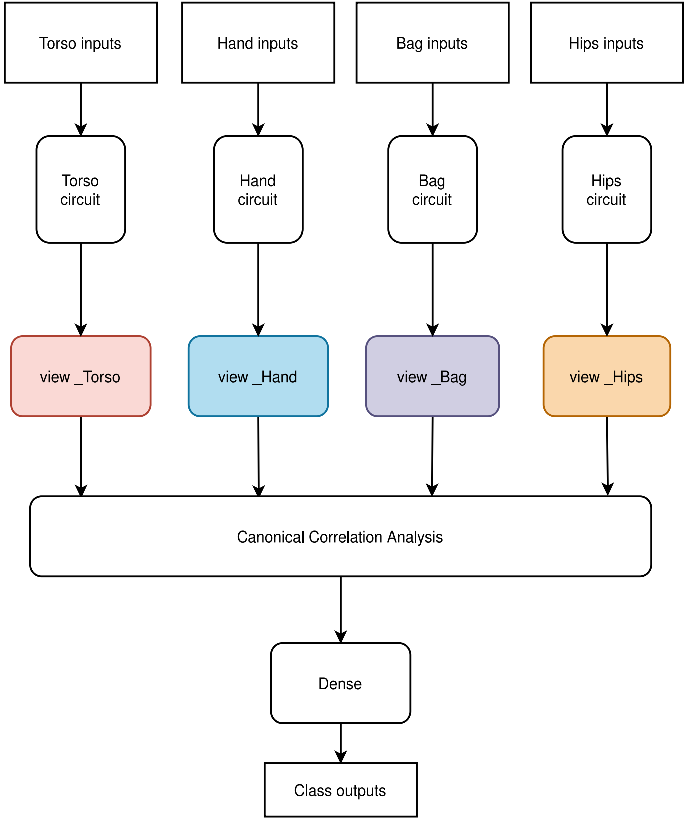

Bias Induced by the Sensor’s Position

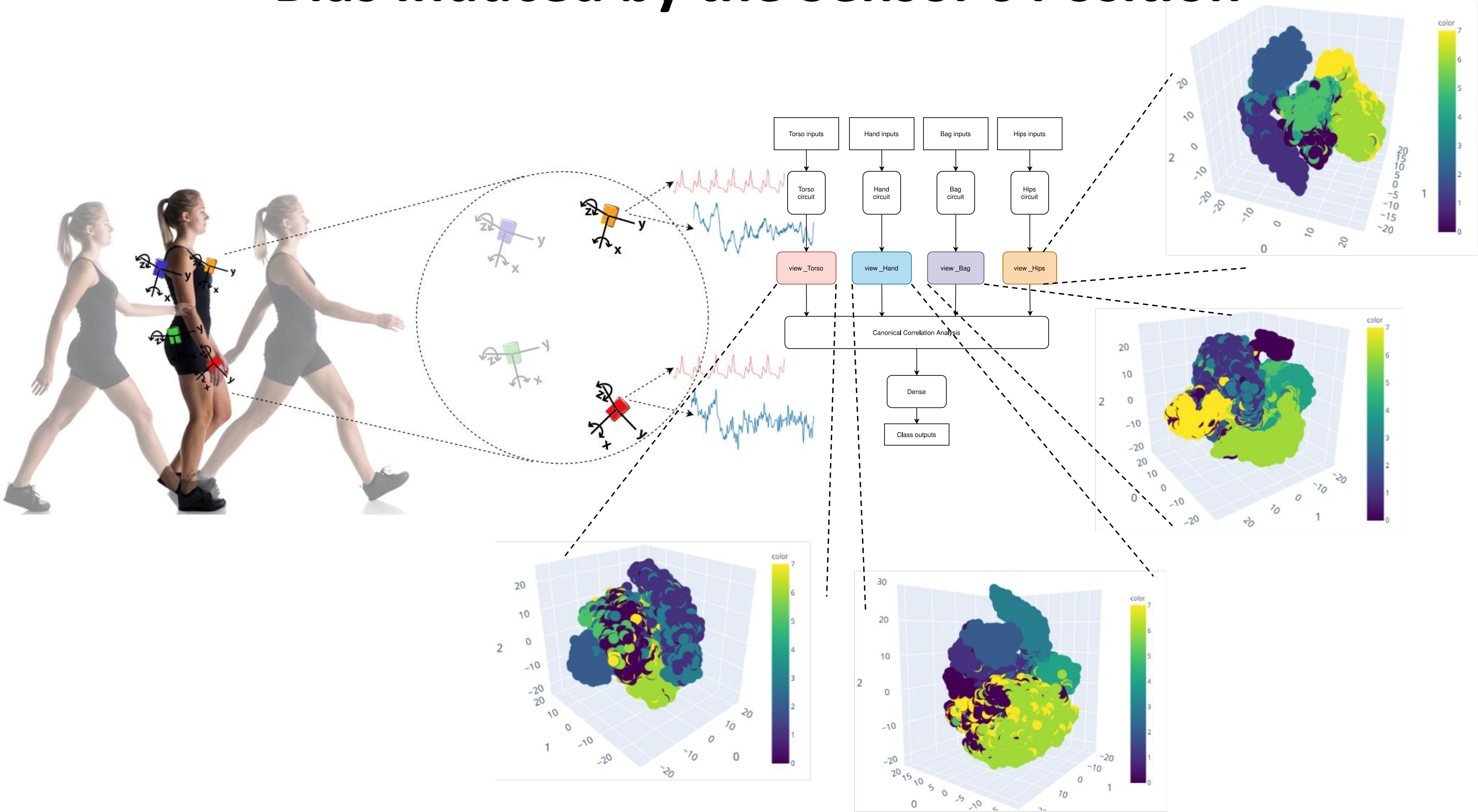

Abstraction
of the sensor's position

Abstraction of the Sensor’s Position

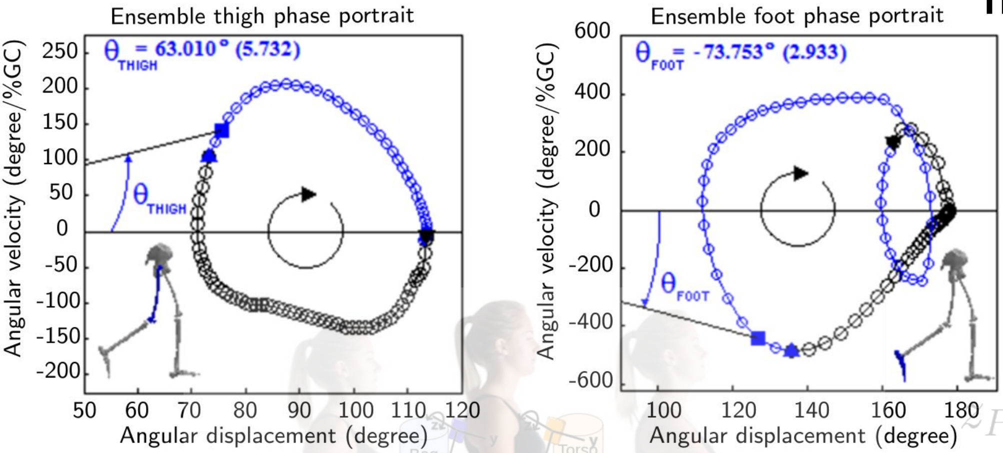

Translational and **circular** movements:

- Discriminating between *walking* and *running* can be based simply on the translational components since there is a greater displacement relative to the environment;
- Discriminating between *running* and *cycling* can be done using the cyclic components since the hand remains relatively static while cycling.

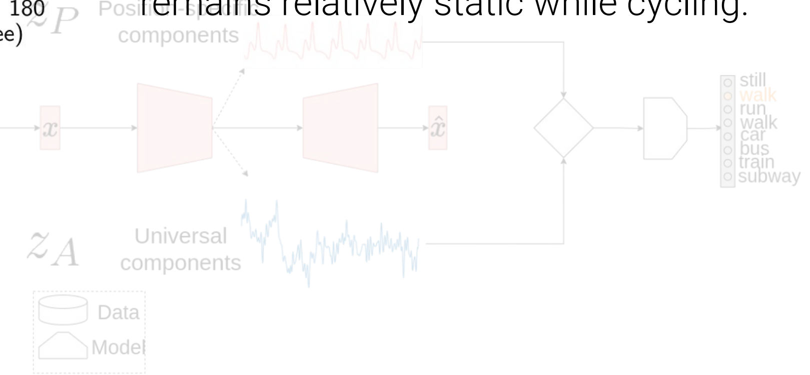

Abstraction of the Sensor's Position

The goal is to build a transformation through which each sensor $s \in S$ will have the ability to **disentangle** the intertwined data streams $\mathbf{x}$ between the **local** and **universal** component by projecting them into two distinct representations z_A and z_P.

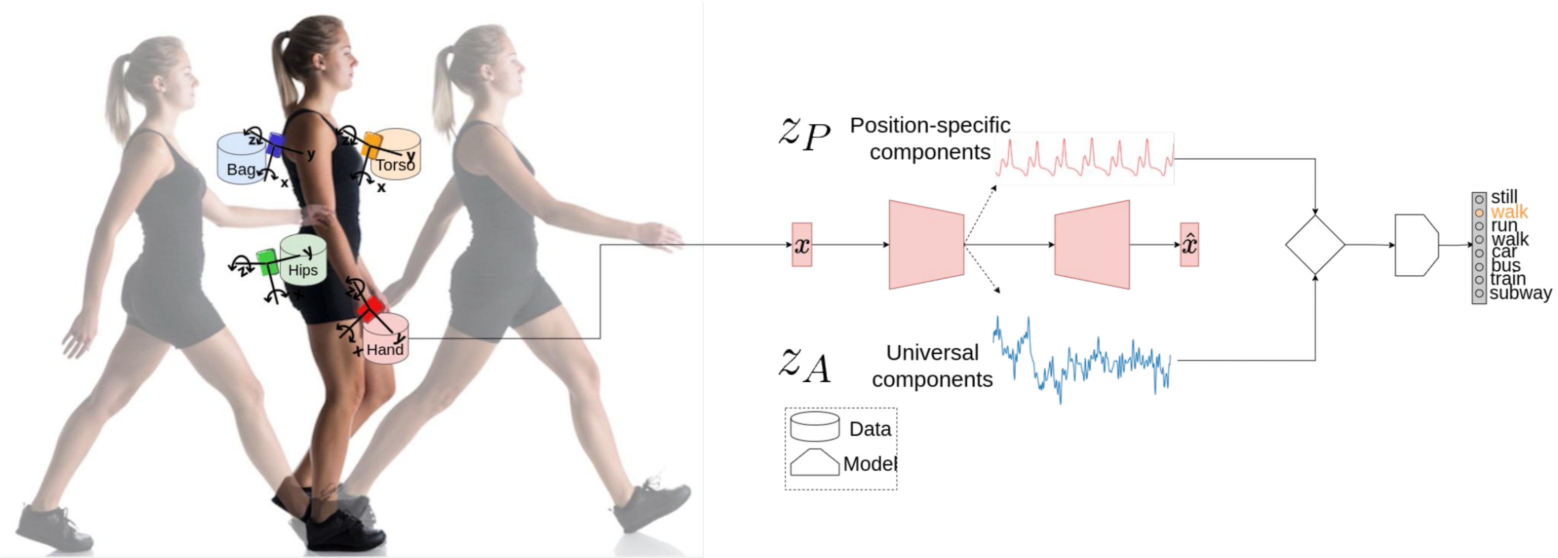

Disentanglement Approaches

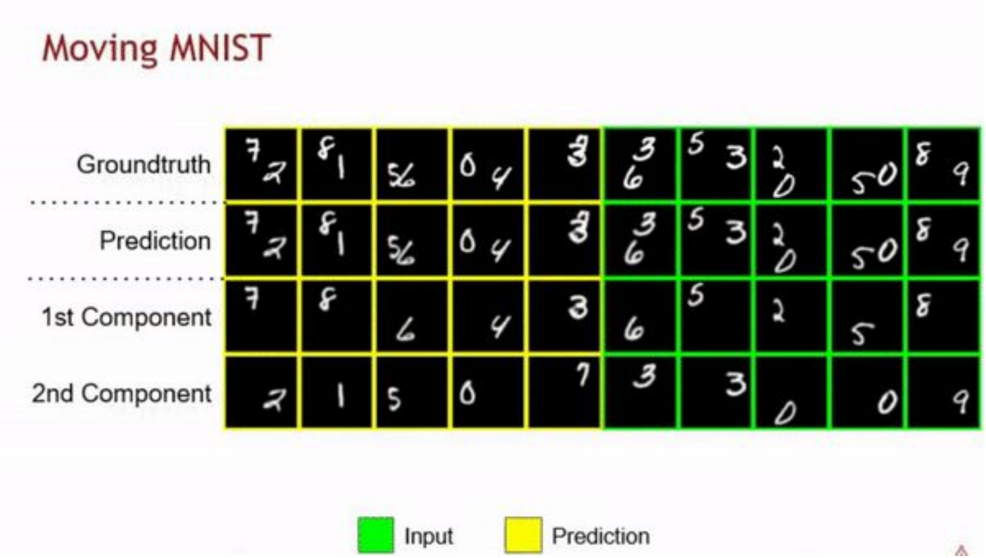

Hsieh, Jun-Ting, et al. "Learning to decompose and disentangle representations for video prediction." *NeurIPS* 2018.

Disentanglement Approaches

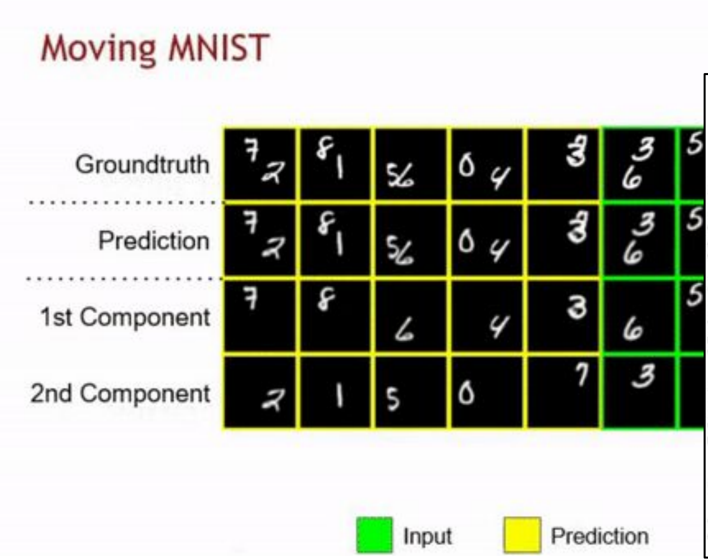

dSprites dataset

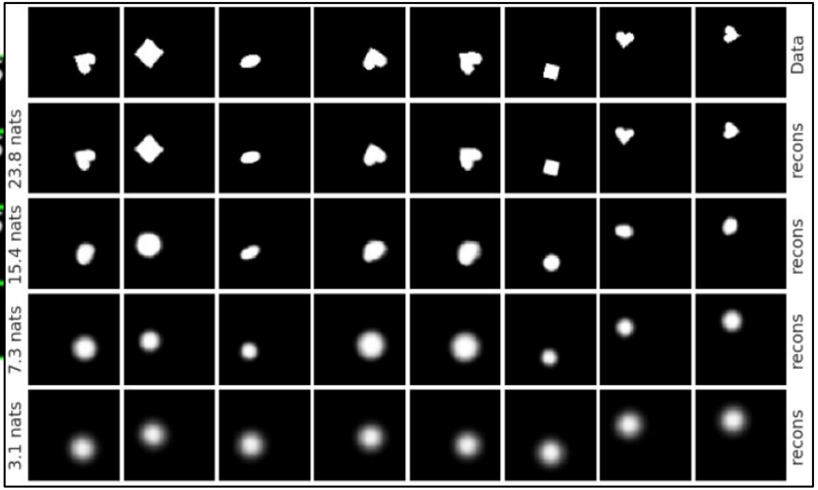

Matthey, L., Higgins, I., Hassabis, D., & Lerchner, A. dSprites: Disentanglement testing sprites dataset, 2017. URL https://github.com/deepmind/dsprites-dataset.

Disentanglement Approaches

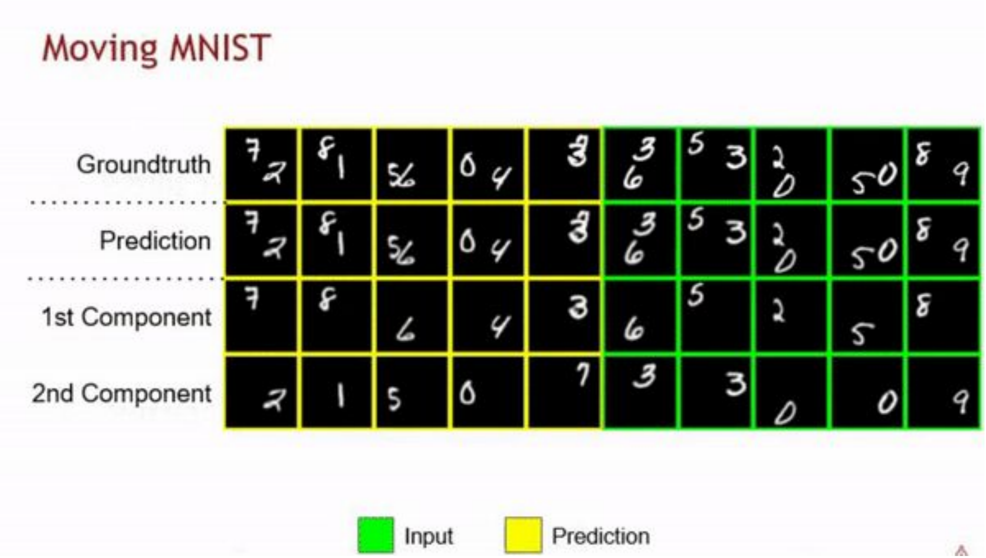

Explicit separation of the components of the latent representation:

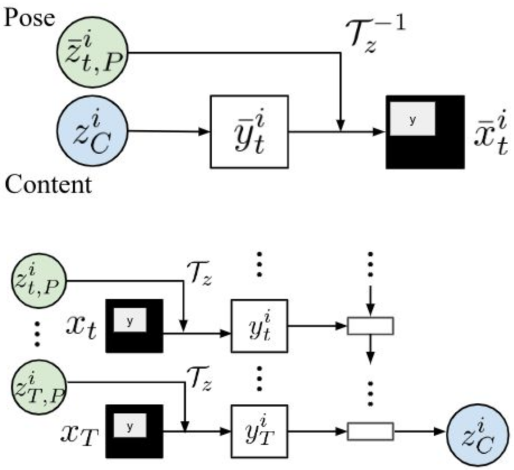

Hsieh, Jun-Ting, et al. "Learning to decompose and disentangle representations for video prediction." *NeurIPS* 2018.

Disentanglement Approaches

dSprites dataset

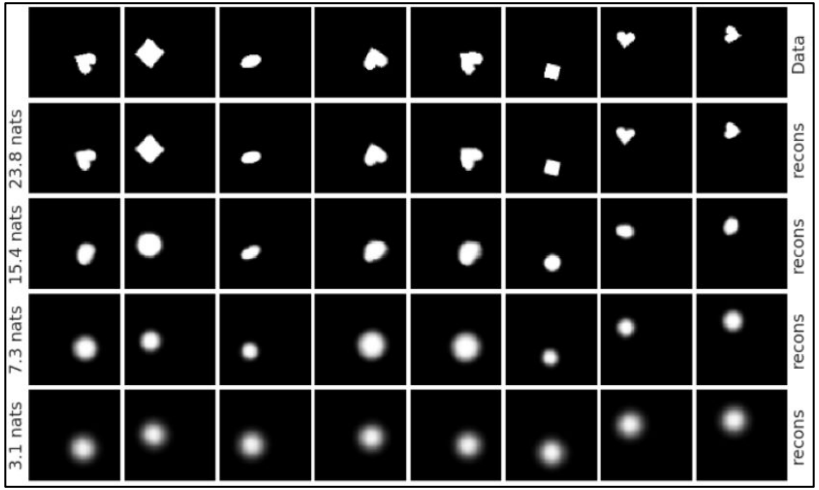

Implicit separation (or decomposition) of the components of the latent representations using the β-VAE

$$L(\theta, \varphi; x, z) = \mathbb{E}_{q_\varphi}(z|x)[\log p_\theta(x|z)] - \beta D_{KL}(q_\varphi(z|x)||p(z))$$

Burgess, Christopher P., et al. "Understanding disentangling in beta -VAE." *arXiv preprint arXiv:1804.03599* 2018.
Matthey, L., Higgins, I., Hassabis, D., & Lerchner, A. dSprites: Disentanglement testing sprites dataset, 2017. URL https://github.com/deepmind/dsprites-dataset.

Disentanglement Approaches

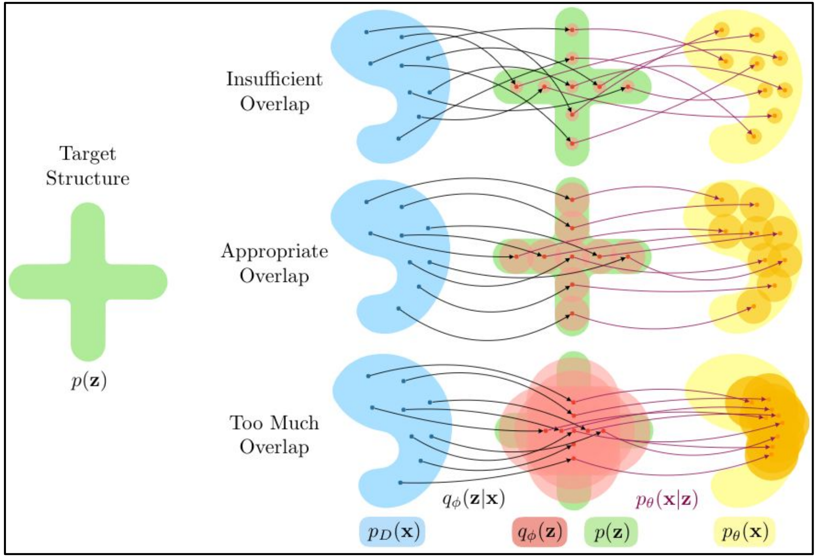

Imposing a particular structure to the learned representations:

$$
\begin{aligned}
L(\theta, \varphi; x, z) = \\
&\mathbb{E}_{q_\varphi}(z|x)[\log p_\theta(x|z)] \\
&- \beta D_{KL}(q_\varphi(z|x)||p(z)) \\
&- \alpha D_{KL}(q_\varphi(z)||p(z))
\end{aligned}
$$

Mathieu, Emile, et al. "Disentangling disentanglement in variational autoencoders." *ICML* 2019.

Disentanglement Approaches

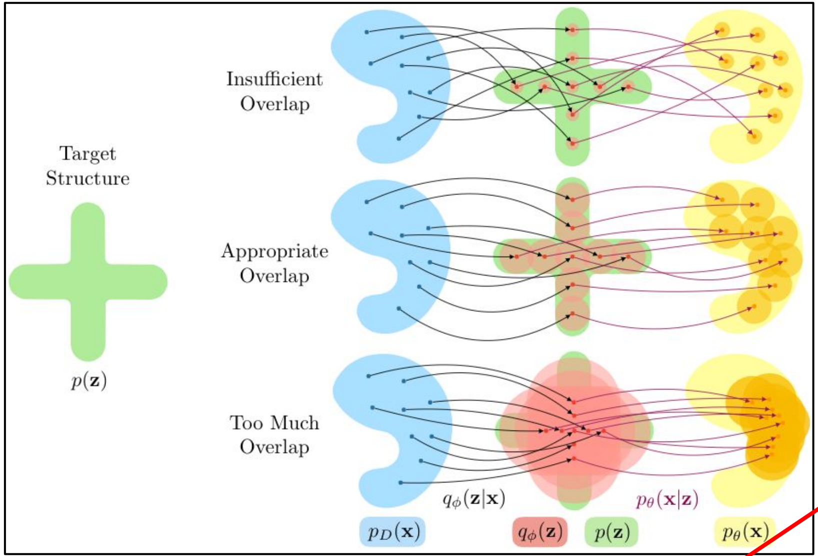

Imposing a particular structure to the learned representations:

Reconstruction error

$$L(\theta, \varphi; x, z) = \mathbb{E}_{q_\varphi}(z|x)[\log p_\theta(x|z)] - \beta D_{KL}(q_\varphi(z|x)||p(z)) - \alpha D_{KL}(q_\varphi(z)||p(z))$$

Divergence between the posterior distribution and the target structure

Constraint imposing sparsity of the learned representations

Mathieu, Emile, et al. "Disentangling disentanglement in variational autoencoders." *ICML* 2019.

Multi-Level Learning Framework

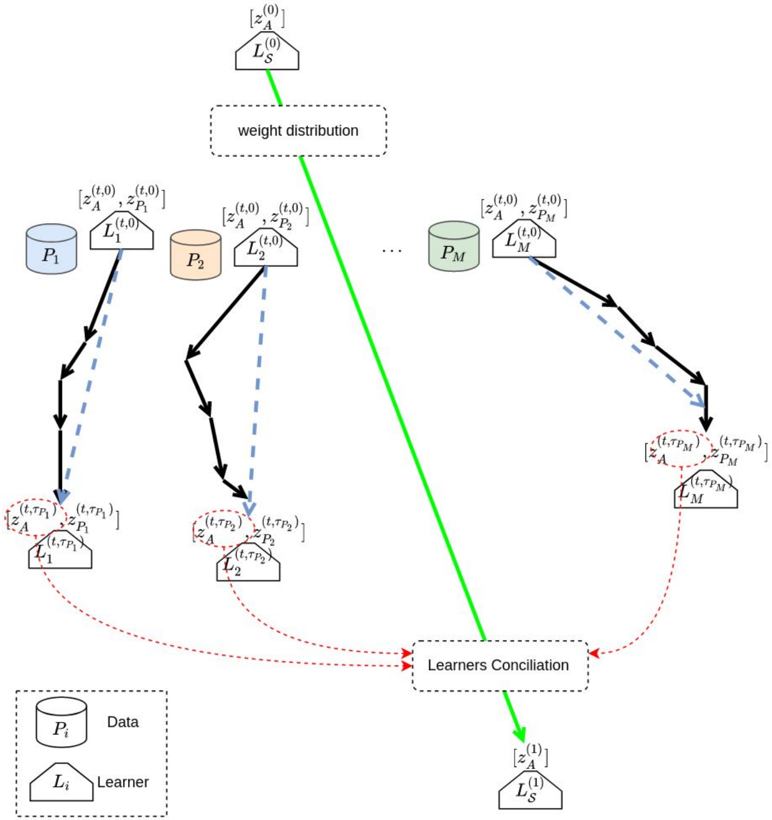

Local learners

- specific to each position of the sensor deployment
- decomposition of signal/data into position-specific and universal (mutualizable) components

Multi-Level Learning Framework

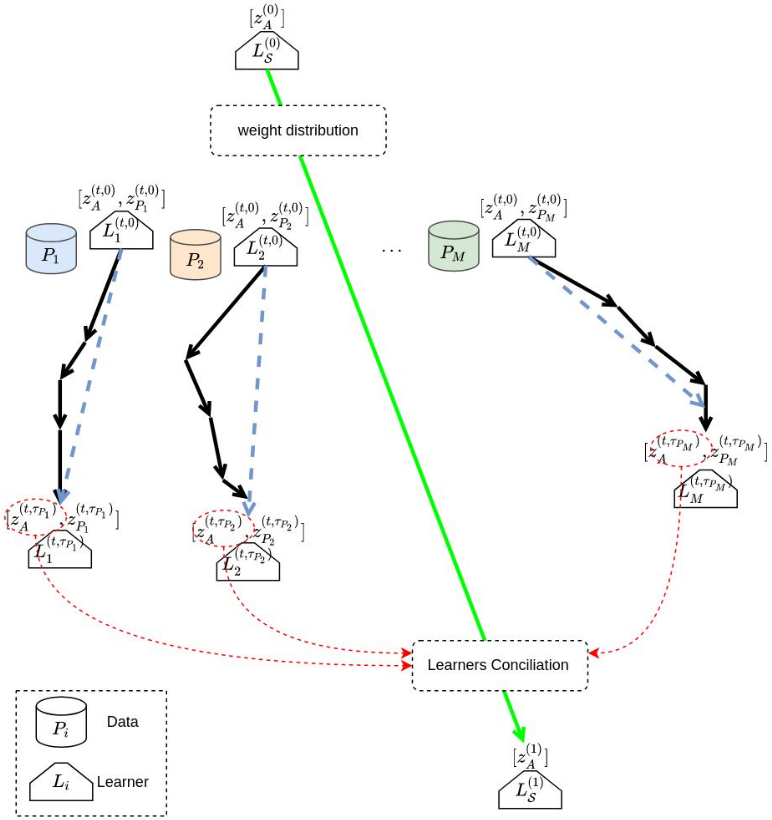

Local learners

- specific to each position of the sensor deployment
- decomposition of signal/data into position-specific and universal (mutualizable) components

The objective of the local learner L_p can be formalized as the expected loss over the data distribution of the position p:

$$f_p(w_p) = \mathbb{E}_{\xi_p}[\tilde{f}_p(w_p; \xi_p)]$$

where ξ_p is a random data sample drawn according to the distribution of position p and $\tilde{f}_p(w_p; \xi_p)$ is a loss function corresponding to this sample while w_p are the learner's weights.

Multi-Level Learning Framework

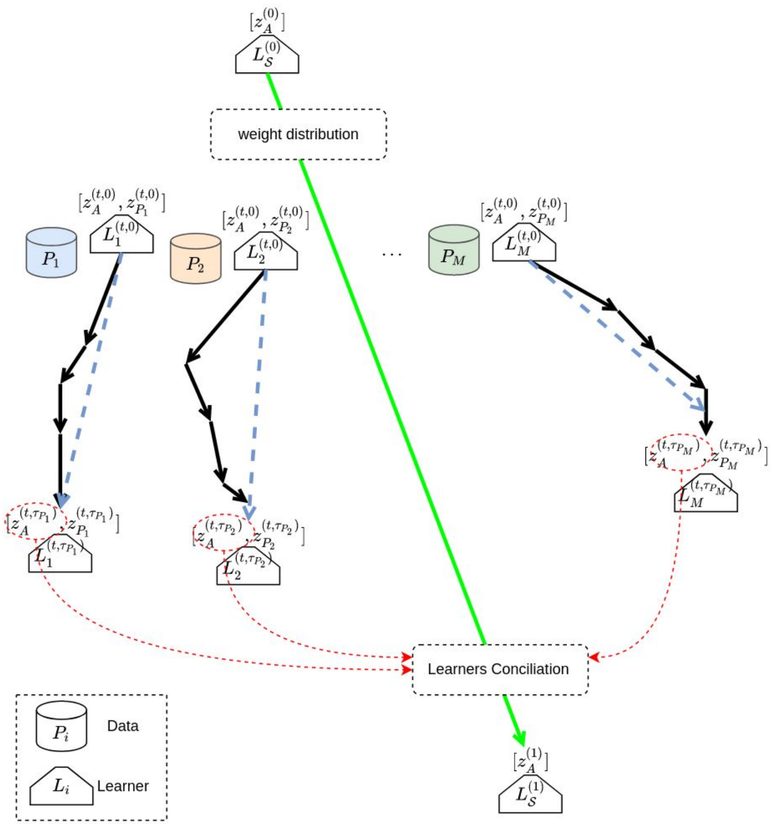

Local learners

- specific to each position of the sensor deployment
- decomposition of signal/data into position-specific and universal (mutualizable) components

Referential (central) learner

- conciliation of the different perspectives

$$\min_{w \in \mathbb{R}^d} \left\{ F(w) := \sum_{p=1}^{M} \alpha_p \times f_p(w_p) \right\} \; with \; \sum_{p=1}^{M} \alpha_p = 1$$

Multi-Level Learning Framework

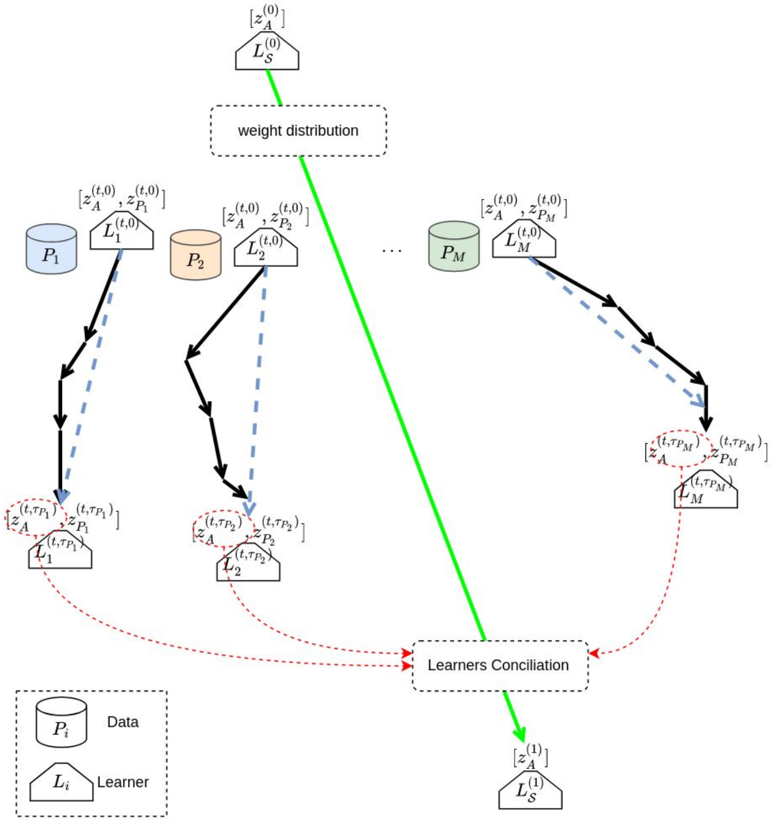

Local learners

- specific to each position of the sensor deployment
- decomposition of signal/data into position-specific and universal (mutualizable) components

Referential (central) learner

- conciliation of the different perspectives
- alignment of the universal representations

$$\min_{w \in \mathbb{R}^d} \left\{ F(w) := \sum_{p=1}^{M} \alpha_p \times f_p(w_p) \right\} \; with \; \sum_{p=1}^{M} \alpha_p = 1$$

$$\min_{w \in \mathbb{R}^d} \left\{ F(w) = \frac{1}{M} \sum_{p=1}^{M} F_p(w_p) \right\}, \; F_p(w_p) = \min_{w \in \mathbb{R}^d} \left\{ f_p(w_p) + \lambda R(z_{iA}, z_A^{(t)}) \right\}$$

Multi-Level Learning Framework

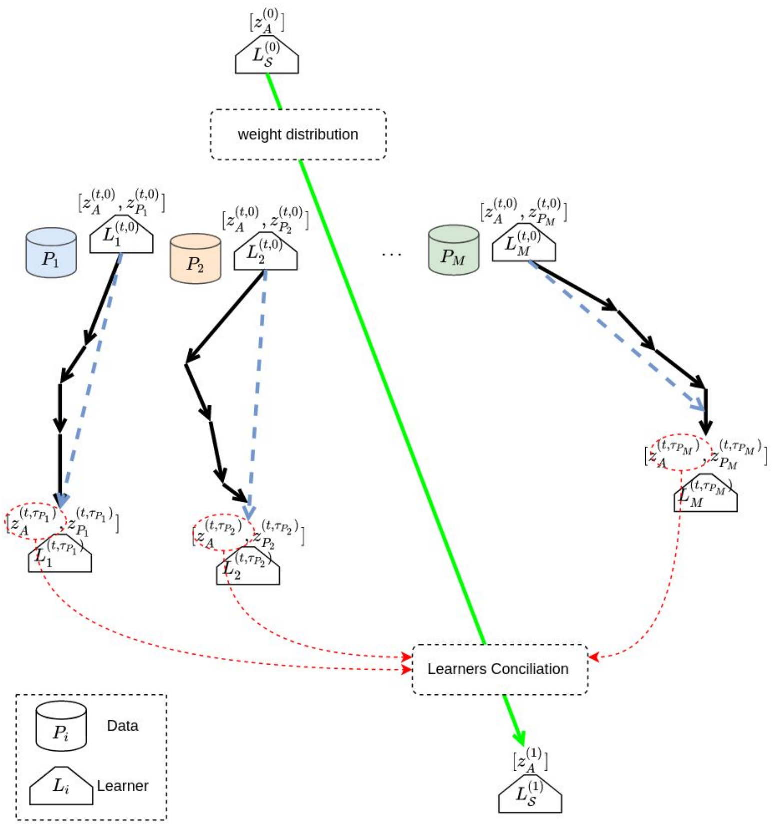

Local learners

- specific to each position of the sensor deployment
- decomposition of signal/data into position-specific and universal (mutualizable) components

Referential (central) learner

- conciliation of the different perspectives
- alignment of the universal representations

$$\min_{w \in \mathbb{R}^d} \left\{ F(w) := \sum_{p=1}^{M} \alpha_p \times f_p(w_p) \right\} \; with \; \sum_{p=1}^{M} \alpha_p = 1$$

$$\min_{w \in \mathbb{R}^d} \left\{ F(w) = \frac{1}{M} \sum_{p=1}^{M} F_p(w_p) \right\}, \; F_p(w_p) = \min_{w \in \mathbb{R}^d} \left\{ f_p(w_p) + \boxed{\lambda R(z_{iA}, z_A^{(t)})} \right\}$$

Multi-Level Learning Framework

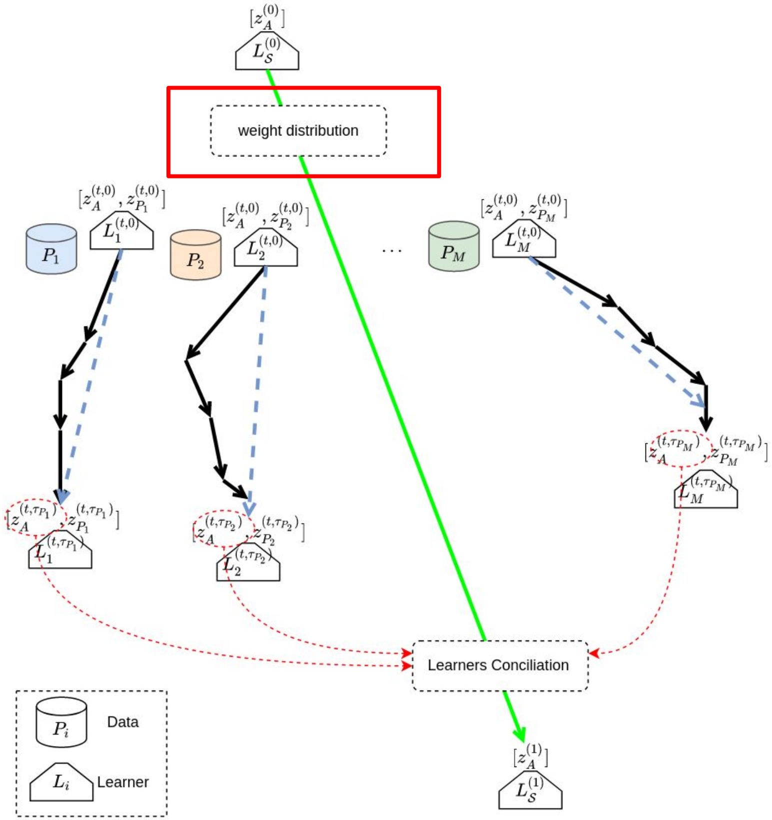

Initialization of referential learner weights and their distribution to local learners

Multi-Level Learning Framework

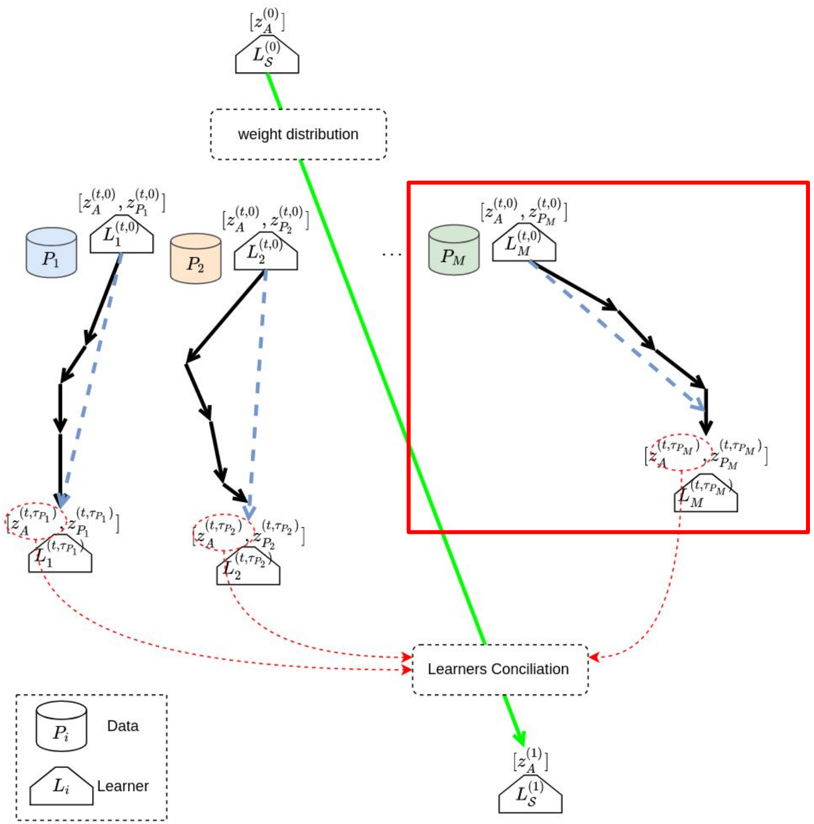

At the step t of communication round, each local learner independently runs τ_p iterations of the local solver, e.g., stochastic gradient descent, starting from the current global model $L_p^{(t,0)}$ until the step $L_p^{(t,\tau_p)}$ to optimize its own local objective (see the black arrows).

Multi-Level Learning Framework

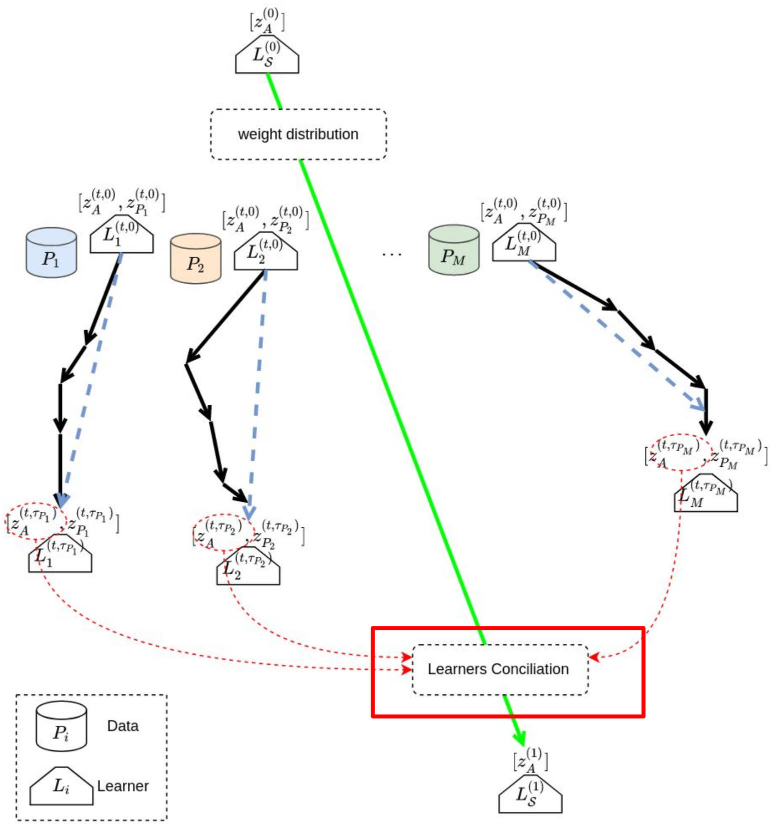

$$w^{(t+1,0)} - w^{(t,0)} = \sum_{p=1}^{M} \alpha_p \Delta_p^{(t)} = -\sum_{p=1}^{M} \alpha_p \cdot \eta \sum_{k=0}^{\tau_p - 1} g_p(w_p^{(t,k)})$$

where $w_p^{(t,k)}$ denotes client p's model after the k-th local update in the t-th communication round and $\Delta_p^{(t)} = w_p^{(t,\tau_p)} - w_p^{(t,0)}$ denotes the cumulative local progress made by client p at round t. η is the client learning rate and g_p represents the stochastic gradient over a mini-batch of B samples.

Experiments

Experimental Evaluation

(i) Evaluation of the data decomposition process

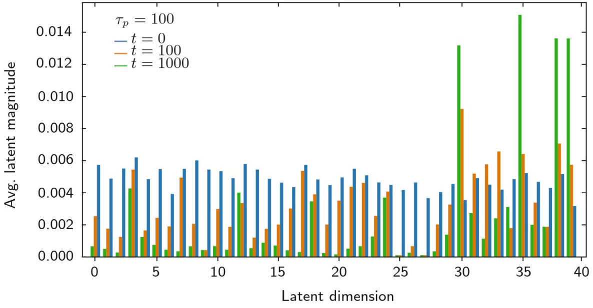

Model	HHAR	Fusion	SHL
DeepConvLSTM	$70.1_{\pm.0018}$	$68.5_{\pm.002}$	$65.3_{\pm.0206}$
DeepSense	$72.0_{\pm.0022}$	$69.1_{\pm.0017}$	$66.5_{\pm.006}$
AttnSense	$76.2_{\pm.0074}$	$70.3_{\pm.0027}$	$68.4_{\pm.03}$
Feature fusion	$72.9_{\pm.004}$	$68.7_{\pm.001}$	$66.8_{\pm.009}$
Corr. align.	$75.8_{\pm.0014}$	$70.2_{\pm.04}$	$69.1_{\pm.015}$
Proposed	$78.3_{\pm.0045}$	$72.8_{\pm.002}$	$74.5_{\pm.0133}$

(ii) Performances comparison

(iii) Inference configurations

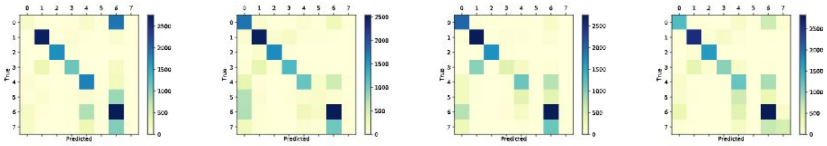

(a) $z_A; z_{Torso}$ (b) $z_A; z_{Hand}$ (c) $z_A; z_{Bag}$ (d) $z_A; z_{Hips}$

Experimental Setup

- Representative datasets
  - SHL, HHAR, Fusion datasets;
  - Multimodal and multilocation sensor data;
- Baselines
  - DeepConvLSTM, DeepSense, AttnSense
  - Feature fusion, Correlation alignment
- Performance evaluation
  - Meta-segmented cross-validation
  - F1-score

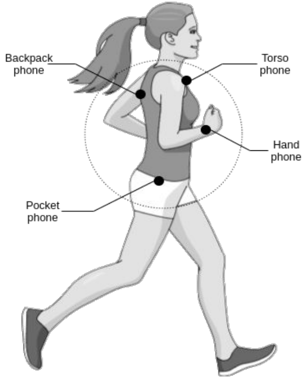

Topology of the wearable sensors deployment in a real-world application

H Gjoreski et al. IEEE Access 6, 2018
Stisen, Allan, et al. ACM SenSys. 2015
Shoaib, Muhammad, et al. Sensors, 2014

Experimental Setup

- Representative datasets
  - SHL, HHAR, Fusion datasets;
  - Multimodal and multilocation sensor data;
- Baselines
  - DeepConvLSTM, DeepSense, AttnSense
  - Feature fusion, Correlation alignment
- Performance evaluation
  - Meta-segmented cross-validation
  - F1-score

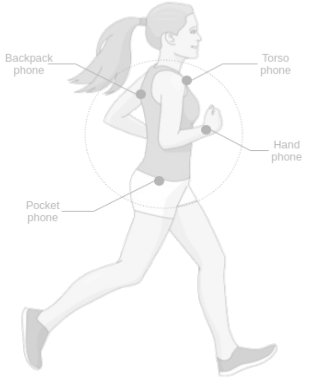

Topology of the wearable sensors deployment in a real-world application

Ordóñez, Francisco Javier, and Daniel Roggen. Sensors, 2016.
Yao, Shuochao, et al. World Wide Web, 2017.
Ma, Haojie, et al. IJCAI, 2019.

Experimental Evaluation

(i) Evaluation of the data decomposition process

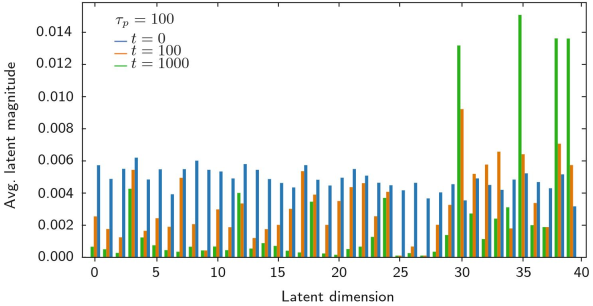

Model	HHAR	Fusion	SHL
DeepConvLSTM	$70.1_{\pm .0018}$	$68.5_{\pm .002}$	$65.3_{\pm .0206}$
DeepSense	$72.0_{\pm .0022}$	$69.1_{\pm .0017}$	$66.5_{\pm .006}$
AttnSense	$76.2_{\pm .0074}$	$70.3_{\pm .0027}$	$68.4_{\pm .03}$
Feature fusion	$72.9_{\pm .004}$	$68.7_{\pm .001}$	$66.8_{\pm .009}$
Corr. align.	$75.8_{\pm .0014}$	$70.2_{\pm .04}$	$69.1_{\pm .015}$
Proposed	$78.3_{\pm .0045}$	$72.8_{\pm .002}$	$74.5_{\pm .0133}$

(ii) Performances comparison

(iii) Inference configurations

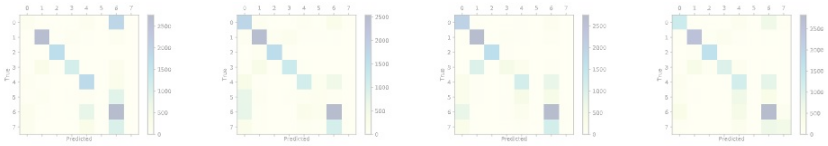

(a) $z_A; z_{Torso}$ (b) $z_A; z_{Hand}$ (c) $z_A; z_{Bag}$ (d) $z_A; z_{Hips}$

Evaluation of the Data Decomposition Process

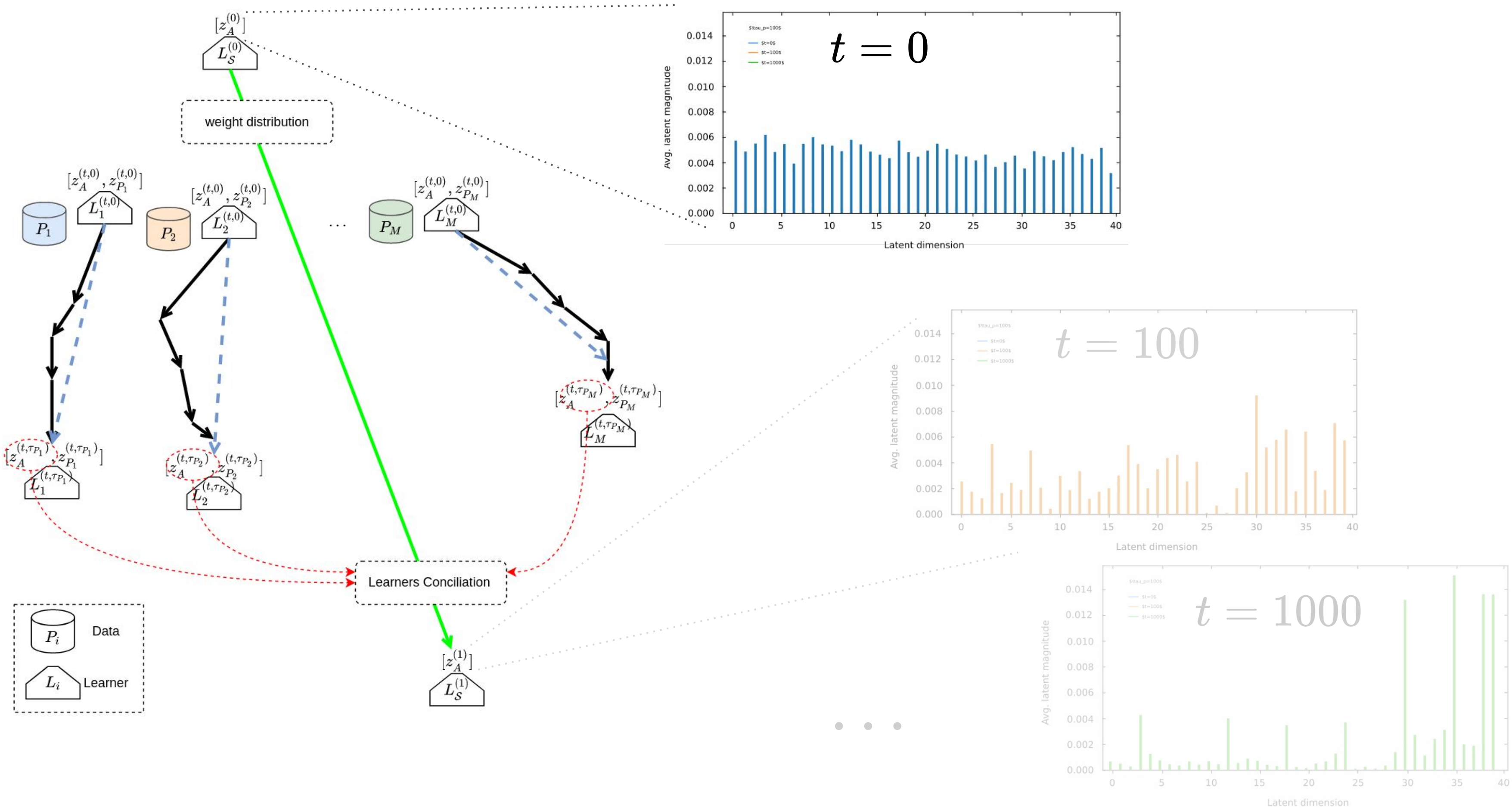

Evaluation of the Data Decomposition Process

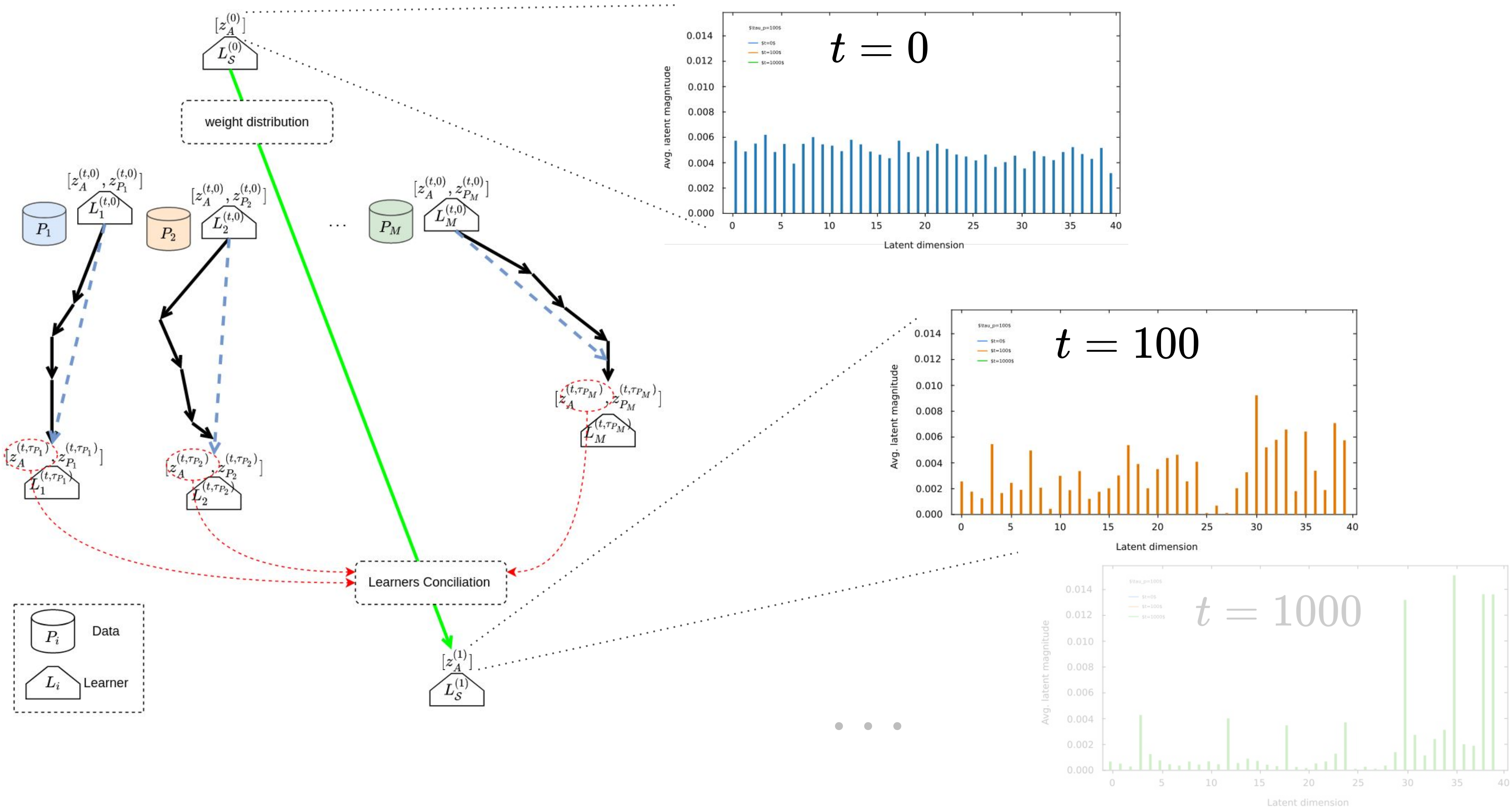

Evaluation of the Data Decomposition Process

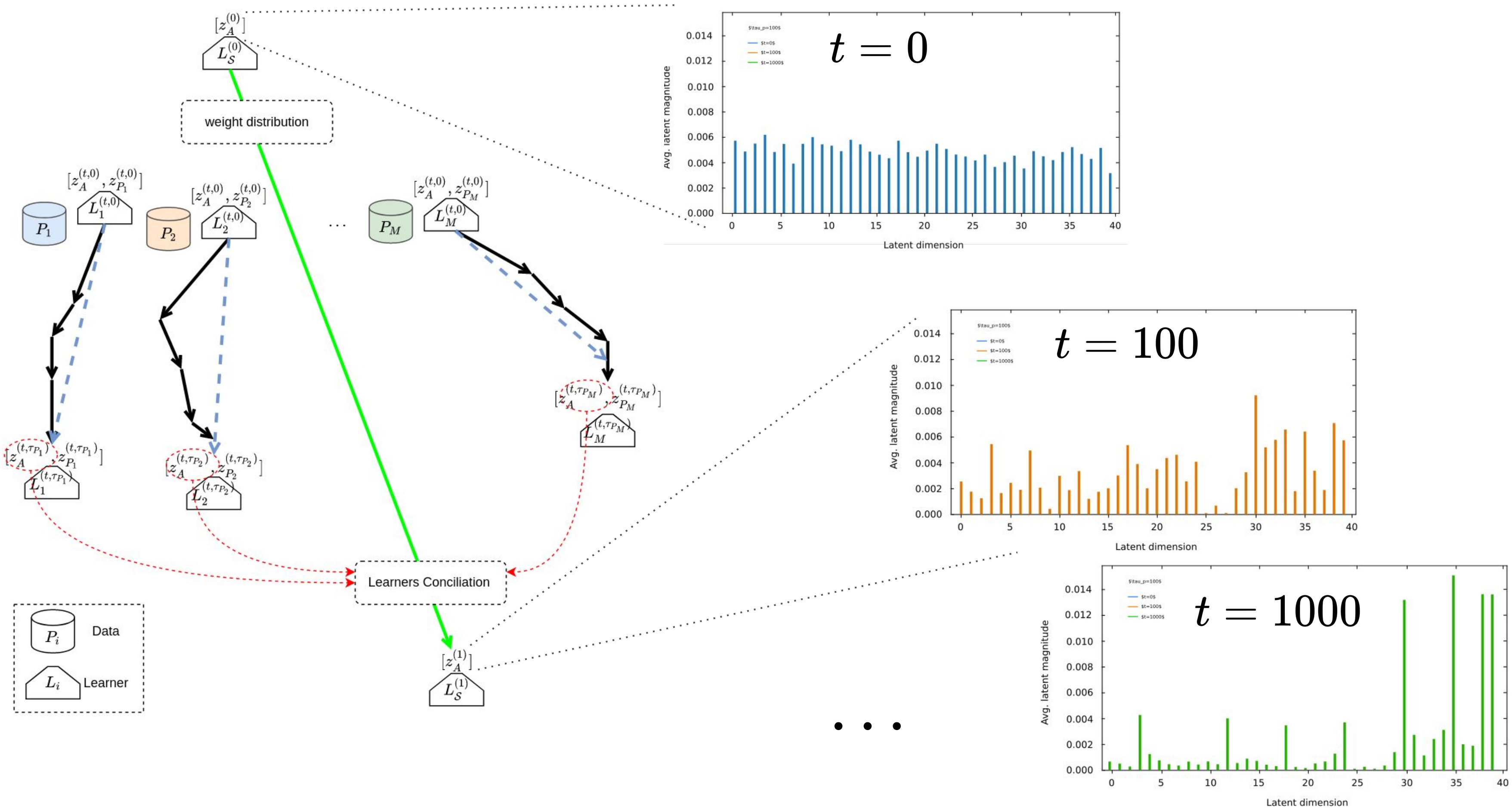

Experimental Evaluation

(i) Evaluation of the data decomposition process

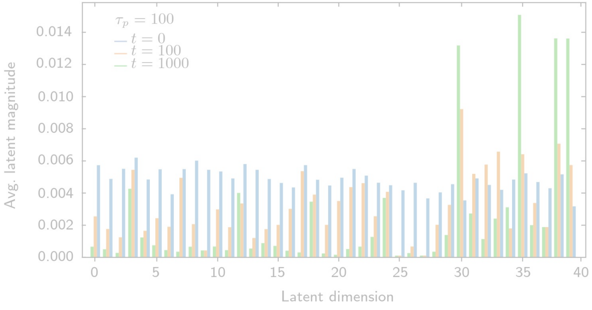

Model	HHAR	Fusion	SHL
DeepConvLSTM	$70.1_{\pm.0018}$	$68.5_{\pm.002}$	$65.3_{\pm.0206}$
DeepSense	$72.0_{\pm.0022}$	$69.1_{\pm.0017}$	$66.5_{\pm.006}$
AttnSense	$76.2_{\pm.0074}$	$70.3_{\pm.0027}$	$68.4_{\pm.03}$
Feature fusion	$72.9_{\pm.004}$	$68.7_{\pm.001}$	$66.8_{\pm.009}$
Corr. align.	$75.8_{\pm.0014}$	$70.2_{\pm.04}$	$69.1_{\pm.015}$
Proposed	$78.3_{\pm.0045}$	$72.8_{\pm.002}$	$74.5_{\pm.0133}$

(ii) Performances comparison

(iii) Inference configurations

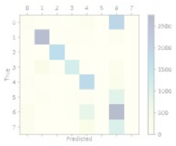
(a) $z_A; z_{Torso}$

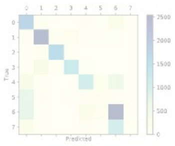
(b) $z_A; z_{Hand}$

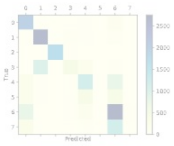
(c) $z_A; z_{Bag}$

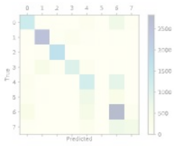
(d) $z_A; z_{Hips}$

Performance Comparison

Model	HHAR	Fusion	SHL
DeepConvLSTM	70.1$\pm$.0018	68.5$\pm$.002	65.3$\pm$.0206
DeepSense	72.0$\pm$.0022	69.1$\pm$.0017	66.5$\pm$.006
AttnSense	76.2$\pm$.0074	70.3$\pm$.0027	68.4$\pm$.03
Feature fusion	72.9$\pm$.004	68.7$\pm$.001	66.8$\pm$.009
Corr. align.	75.8$\pm$.0014	70.2$\pm$.04	69.1$\pm$.015
Proposed	78.3$\pm$.0045	72.8$\pm$.002	74.5$\pm$.0133

Performance Comparison

Model	HHAR	Fusion	SHL
DeepConvLSTM	70.1$\pm$.0018	68.5$\pm$.002	65.3$\pm$.0206
DeepSense	72.0$\pm$.0022	69.1$\pm$.0017	66.5$\pm$.006
AttnSense	76.2$\pm$.0074	70.3$\pm$.0027	68.4$\pm$.03
Feature fusion	72.9$\pm$.004	68.7$\pm$.001	66.8$\pm$.009
Corr. align.	75.8$\pm$.0014	70.2$\pm$.04	69.1$\pm$.015
Proposed	78.3$\pm$.0045	72.8$\pm$.002	74.5$\pm$.0133

Performance Comparison

Model	HHAR	Fusion	SHL
DeepConvLSTM	$70.1_{\pm .0018}$	$68.5_{\pm .002}$	$65.3_{\pm .0206}$
DeepSense	$72.0_{\pm .0022}$	$69.1_{\pm .0017}$	$66.5_{\pm .006}$
AttnSense	$76.2_{\pm .0074}$	$70.3_{\pm .0027}$	$68.4_{\pm .03}$
Feature fusion	$72.9_{\pm .004}$	$68.7_{\pm .001}$	$66.8_{\pm .009}$
Corr. align.	$75.8_{\pm .0014}$	$70.2_{\pm .04}$	$69.1_{\pm .015}$
Proposed	$78.3_{\pm .0045}$	$72.8_{\pm .002}$	$74.5_{\pm .0133}$

Experimental Evaluation

(i) Evaluation of the data decomposition process

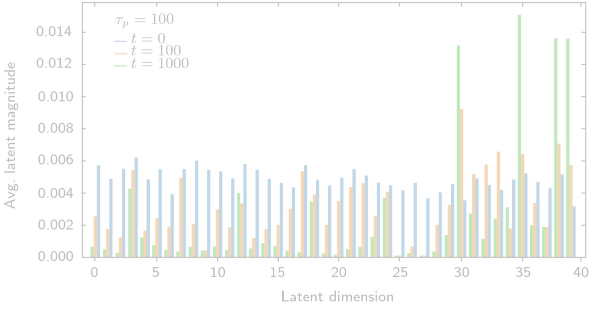

(ii) Performances comparison

Model	HHAR	Fusion	SHL
DeepConvLSTM	$70.1_{\pm.0018}$	$68.5_{\pm.002}$	$65.3_{\pm.0206}$
DeepSense	$72.0_{\pm.0022}$	$69.1_{\pm.0017}$	$66.5_{\pm.006}$
AttnSense	$76.2_{\pm.0074}$	$70.3_{\pm.0027}$	$68.4_{\pm.03}$
Feature fusion	$72.9_{\pm.004}$	$68.7_{\pm.001}$	$66.8_{\pm.009}$
Corr. align.	$75.8_{\pm.0014}$	$70.2_{\pm.04}$	$69.1_{\pm.015}$
Proposed	$78.3_{\pm.0045}$	$72.8_{\pm.002}$	$74.5_{\pm.0133}$

(iii) Inference configurations

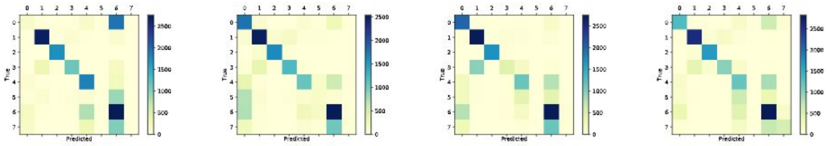

(a) $z_A; z_{Torso}$ (b) $z_A; z_{Hand}$ (c) $z_A; z_{Bag}$ (d) $z_A; z_{Hips}$

Basic Inference Configurations

Config.	Recognition Performances±std.			
	Bag	*Hand*	*Hips*	*Torso*
Baseline (no sep.)	63.79 ± .0089	63.86 ± .0014	65.70 ± .0126	60.61 ± .0072
Universal comp.				
w/o conciliation	66.17 ± .0224	65.26 ± .0147	66.12 ± .0035	62.47 ± .013
w/ conciliation	66.97 ± .016	67.8 ± .0015	67.84 ± .0354	63.12 ± .01
Pos.-specific comp.				
w/o conciliation	64.2 ± .3	66.17 ± .007	67.9 ± .0026	61.32± .087
w/ conciliation	65.66 ± .029	68.94 ± .03	70.45 ± .07	61.15 ± .029

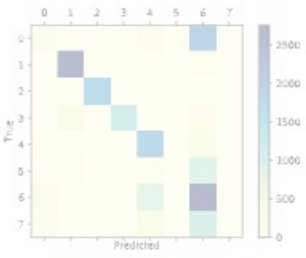

(a) $z_A; z_{Torso}$

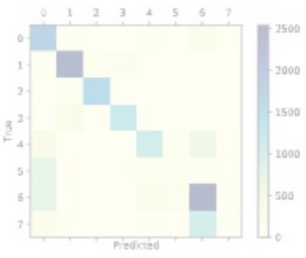

(b) $z_A; z_{Hand}$

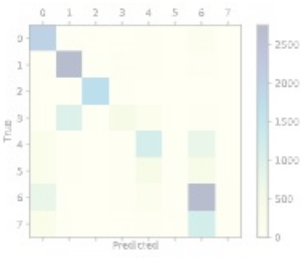

(c) $z_A; z_{Bag}$

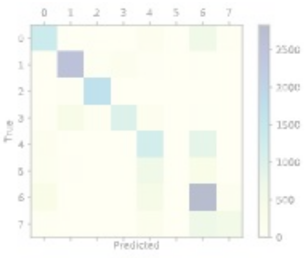

(d) $z_A; z_{Hips}$

Basic Inference Configurations

Config.	Recognition Performances±std.			
	Bag	*Hand*	*Hips*	*Torso*
Baseline (no sep.)	63.79 ± .0089	63.86 ± .0014	65.70 ± .0126	60.61 ± .0072
Universal comp.				
w/o conciliation	66.17 ± .0224	65.26 ± .0147	66.12 ± .0035	62.47 ± .013
w/ conciliation	66.97 ± .016	67.8 ± .0015	67.84 ± .0354	63.12 ± .01
Pos.-specific comp.				
w/o conciliation	64.2 ± .3	66.17 ± .007	67.9 ± .0026	61.32± .087
w/ conciliation	65.66 ± .029	68.94 ± .03	70.45 ± .07	61.15 ± .029

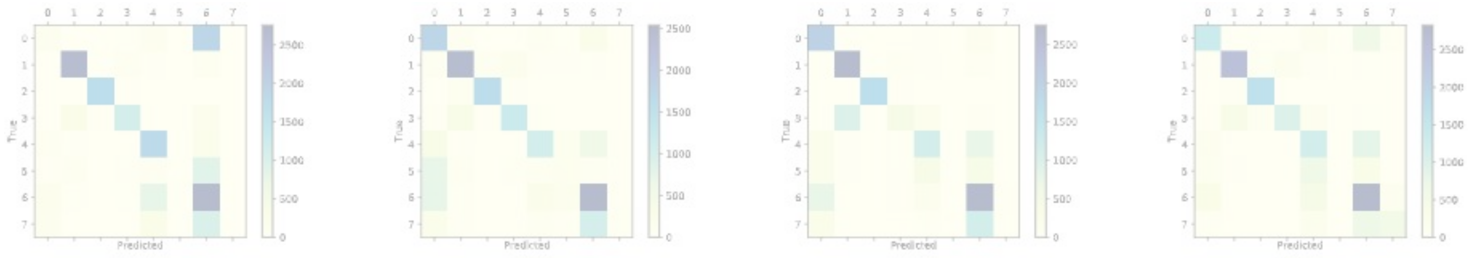

(a) $z_A; z_{Torso}$ (b) $z_A; z_{Hand}$ (c) $z_A; z_{Bag}$ (d) $z_A; z_{Hips}$

Basic Inference Configurations

Config.	Recognition Performances±std.			
	Bag	*Hand*	*Hips*	*Torso*
Baseline (no sep.)	63.79 ± .0089	63.86 ± .0014	65.70 ± .0126	60.61 ± .0072
Universal comp.				
w/o conciliation	66.17 ± .0224	65.26 ± .0147	66.12 ± .0035	62.47 ± .013
w/ conciliation	66.97 ± .016	67.8 ± .0015	67.84 ± .0354	63.12 ± .01
Pos.-specific comp.				
w/o conciliation	64.2 ± .3	66.17 ± .007	67.9 ± .0026	61.32± .087
w/ conciliation	65.66 ± .029	68.94 ± .03	70.45 ± .07	61.15 ± .029

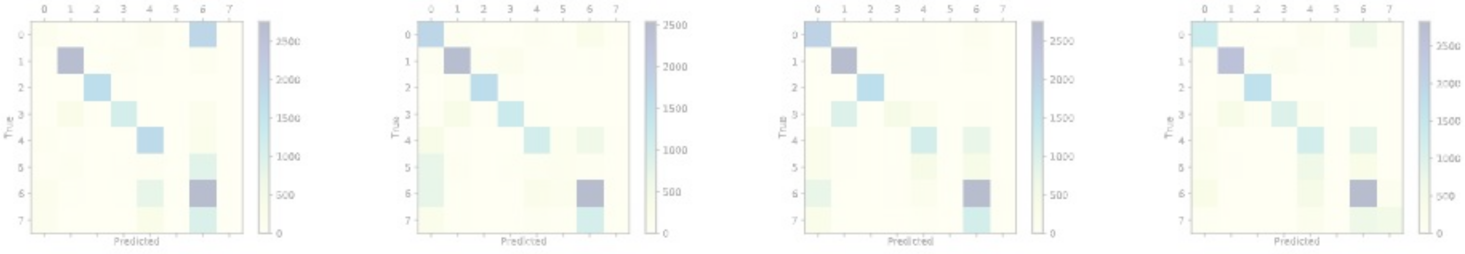

(a) $z_A; z_{Torso}$ (b) $z_A; z_{Hand}$ (c) $z_A; z_{Bag}$ (d) $z_A; z_{Hips}$

Basic Inference Configurations

Config.	Recognition Performances±std.			
	Bag	*Hand*	*Hips*	*Torso*
Baseline (no sep.)	63.79 ± .0089	63.86 ± .0014	65.70 ± .0126	60.61 ± .0072
Universal comp.				
w/o conciliation	66.17 ± .0224	65.26 ± .0147	66.12 ± .0035	62.47 ± .013
w/ conciliation	66.97 ± .016	67.8 ± .0015	67.84 ± .0354	63.12 ± .01
Pos.-specific comp.				
w/o conciliation	64.2 ± .3	66.17 ± .007	67.9 ± .0026	61.32± .087
w/ conciliation	65.66 ± .029	68.94 ± .03	70.45 ± .07	61.15 ± .029

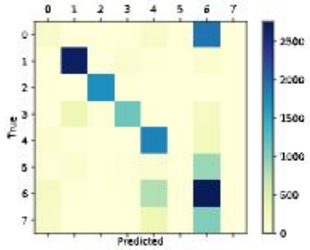

(a) $z_A; z_{Torso}$

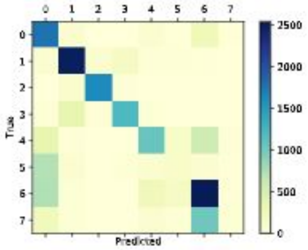

(b) $z_A; z_{Hand}$

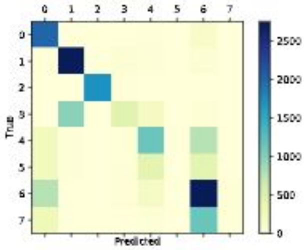

(c) $z_A; z_{Bag}$

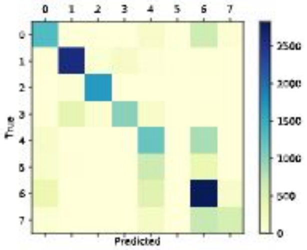

(d) $z_A; z_{Hips}$

Basic Inference Configurations

Config.	Recognition Performances±std.			
	Bag	*Hand*	*Hips*	*Torso*
Baseline (no sep.)	63.79 ± .0089	63.86 ± .0014	65.70 ± .0126	60.61 ± .0072
Universal comp.				
w/o conciliation	66.17 ± .0224	65.26 ± .0147	66.12 ± .0035	62.47 ± .013
w/ conciliation	66.97 ± .016	67.8 ± .0015	67.84 ± .0354	63.12 ± .01
Pos.-specific comp.				
w/o conciliation	64.2 ± .3	66.17 ± .007	67.9 ± .0026	61.32± .087
w/ conciliation	65.66 ± .029	68.94 ± .03	70.45 ± .07	61.15 ± .029

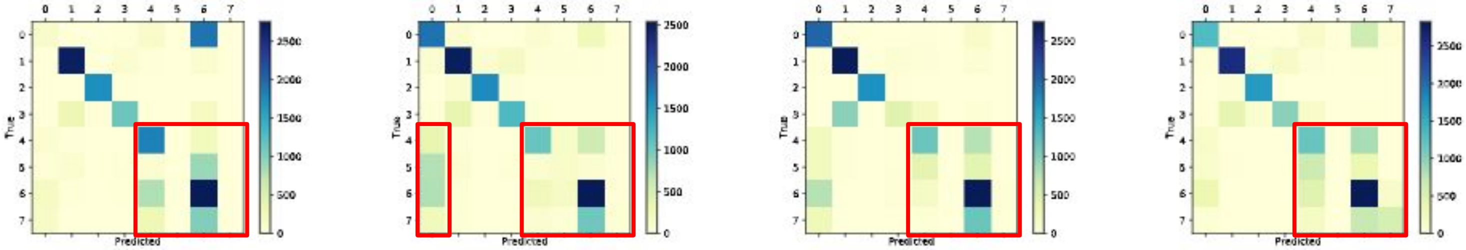

(a) $z_A; z_{Torso}$ (b) $z_A; z_{Hand}$ (c) $z_A; z_{Bag}$ (d) $z_A; z_{Hips}$

~~Basic~~ Suitable Inference Configurations

Config.	*Best Config.*	*Recogn. Perf.±std.*	*mean±std.*
Baselines			
Concat. fusion	-	-	60.24 ± .014
Corr. Alignment	-	-	63.79 ± .032
Activities			
Still	$z_{hi}; z_t$	85.77±0.016	83.26±0.7
Walk	$z_A; z_{ha}$	88.54±0.07	86.74±0.058
Run	z_{ha}	90.51±0.016	89.46±0.03
Bike	$z_A; z_{hi}$	85.62±0.2	83.22±0.086
Car	$z_A; z_{ha}$	78.24±0.058	77.14±0.2
Bus	z_{ha}	78.08±0.022	75.17±0.004
Train	$z_{hi}; z_{hi}$	76.13±0.175	74.88±0.08
Subway	$z_A; z_{ha}; z_t$	75.89±0.009	74.07±0.006

~~Basic~~ Suitable Inference Configurations

Config.	*Best Config.*	*Recogn. Perf.±std.*	*mean±std.*
Baselines			
Concat. fusion	-	-	60.24 ± .014
Corr. Alignment	-	-	63.79 ± .032
Activities			
Still	$z_{hi}; z_t$	85.77±0.016	83.26±0.7
Walk	$z_A; z_{ha}$	88.54±0.07	86.74±0.058
Run	z_{ha}	90.51±0.016	89.46±0.03
Bike	$z_A; z_{hi}$	85.62±0.2	83.22±0.086
Car	$z_A; z_{ha}$	78.24±0.058	77.14±0.2
Bus	z_{ha}	78.08±0.022	75.17±0.004
Train	$z_{hi}; z_{hi}$	76.13±0.175	74.88±0.08
Subway	$z_A; z_{ha}; z_t$	75.89±0.009	74.07±0.006

~~Basic~~ Suitable Inference Configurations

Config.	*Best Config.*	*Recogn. Perf.±std.*	*mean±std.*
Baselines			
Concat. fusion	-	-	60.24 ± .014
Corr. Alignment	-	-	63.79 ± .032
Activities			
Still	$z_{hi}; z_t$	85.77±0.016	83.26±0.7
Walk	$z_A; z_{ha}$	88.54±0.07	86.74±0.058
Run	z_{ha}	90.51±0.016	89.46±0.03
Bike	$z_A; z_{hi}$	85.62±0.2	83.22±0.086
Car	$z_A; z_{ha}$	78.24±0.058	77.14±0.2
Bus	z_{ha}	78.08±0.022	75.17±0.004
Train	$z_{hi}; z_{hi}$	76.13±0.175	74.88±0.08
Subway	$z_A; z_{ha}; z_t$	75.89±0.009	74.07±0.006

Summary

- Sensors distributed in various positions of the space provide rich perspectives that need to be leveraged properly during learning process.
- The information conveyed by these perspectives are not of the same nature: e.g., *Sensor's Position Bias* induce different types of information.
- The proposed approach is able to abstract this bias by decomposing the sensory signals into universal and position-specific components.

contact: hamidi@lipn.univ-paris13.fr
ao@lipn.univ-paris13.fr
LIPN-UMR CNRS 7030, Univ. Sorbonne Paris Nord

Université Sorbonne Paris Nord

contact: hamidi@lipn.univ-paris13.fr
ao@lipn.univ-paris13.fr
LIPN-UMR CNRS 7030, Univ. Sorbonne Paris Nord

Université Sorbonne Paris Nord

PAKDD 2022

THE 26TH PACIFIC-ASIA CONFERENCE ON KNOWLEDGE DISCOVERY AND DATA MINING

MAY, 16-19 CHENGDU, CHINA

西南交通大學 Southwest Jiaotong University